Experimental and Computational Study of HXeY···HX Complexes (X, Y = Cl and Br): An Example of Exceptionally Large Complexation Effect

Antti Lignell,*,† Jan Lundell,‡ Leonid Khriachtchev,† and Markku Räsänen†

Department of Chemistry, P.O. Box 55, FIN-00014 University of Helsinki, Finland, and Department of Chemistry, P.O. Box 35, FIN-40014 University of Jyväskylä, Finland

Received: February 15, 2008; Revised Manuscript Received: March 19, 2008

The complexes of xenon hydrides HXeY (Y = Cl and Br) with hydrogen halides HX (X = Cl and Br) have been studied both computationally and experimentally in a xenon matrix. The experiments revealed three new complexes: HXeBr···HBr, HXeBr···HCl, and HXeCl···HCl. The experimental assignments were done on the basis of the strong H−Xe stretching absorption of HXeY (Y = Cl and Br) molecules and supported by theoretical results. We experimentally obtained monomer-to-complex blue-shifts of this vibrational mode for all the studied systems (up to ∼150 cm^{-1}). The electronic structure calculations revealed three local structures for each HNgY···HX complexes and their computed interaction energies varied between −460 and −2800 cm^{-1}. The computational estimates of the vibrational shifts were in agreement with the experimental values. We also found possible experimental absorption belonging to HXeBr···$(HBr)_2$ trimer and its vibrational shift (+245 cm^{-1}) is similar to the computational estimate of a cyclic ternary complex (+252 cm^{-1}).

Introduction

Intermolecular interactions determine many properties of matter. The interactions with hydrogen bonding are characterized by relatively strong binding energies.[1] In a red-shifting hydrogen bond A···H−X, the stretching vibration frequency of the proton donor H−X decreases upon complexation and its intensity increases. The magnitude of the red-shift has been attributed to the hydrogen bond strength.[2] In contrast to this "normal" behavior, the H−X vibrational frequency of blue-shifting systems increases and the IR-absorption intensity decreases. During the last years, these blue-shifting hydrogen bonds have been under intensive discussion and the physical mechanisms of this unusual behavior have been studied.[3–6]

Noble-gas hydride molecules of the HNgY type (H = hydrogen atom, Ng = noble-gas atom, and Y = electronegative fragment) have been studied both experimentally and computationally since their discovery in 1995.[7,8] These molecules have a strong $(HNg)^+Y^-$ ion-pair character in their equilibrium structure.[8] Because of the relatively weak bonding and large dipole moments of the HNgY molecules, their interactions with other molecules show unusual features. In our experimental and computational study on N_2···HKrCl,[9] the H−Kr stretching vibration exhibits a very large blue-shift (>100 cm^{-1}) upon complexation. We attributed this behavior to the enhanced $(HNg)^+Y^-$ ion-pair character of the HNgY molecule when it interacts with N_2. Blue-shifting hydrogen bonds were also found experimentally for N_2···HArF, N_2···HKrF, and CO_2···HXeCCH complexes.[10,11] Previously, we have pointed out that the blue-shift upon complexation is a "normal" effect for noble-gas hydrides.[10] Importantly, substantial blue-shifts of the H−Ng stretching modes were found for cases with and without hydrogen bond formation directly to the H−Ng entity. As an example, Nemukhin et al. reported highly blue-shifting H−Xe vibrations for HXeOH···$(H_2O)_n$ (n = 1, 2) complexes where H_2O molecules are connected to the OH end of the HXeOH molecule.[12] A substantial number of computational works on HNgY complexes has been published so far.[13–19] The recent computational works on HNgF···HF (Ng = Ar, Kr, and Xe) complexes are most relevant to our present study.[18,19]

In the present work, we study experimentally and computationally the HXeY···HX complexes (X, Y = Cl and Br). For the H−Xe stretching vibrations of the studied systems, we observed blue-shifts upon complexation. We found several experimental absorptions of H−Xe stretching mode and attributed them to various solid-state structures of the HXeY···HX complexes. Electronic structure calculations were applied to support experimental investigations and the obtained counterpoise-corrected interaction energies of different geometries vary between −460 and −2800 cm^{-1}.

Experiment

The HCl/HBr/Xe matrices with different HCl/HBr proportions were prepared by depositing HCl/Xe and HBr/Xe gas mixtures through separate nozzles onto a cold CsI window in a closed-cycle helium cryostat (APD, DE 202A). In most of the experiments, a droplet of H_2SO_4 was inserted into the deposition line to trap water vapor from the sample-gas flow. The substrate temperature during the deposition was 30−60 K, and the typical sample thickness was 100 μm. The absorption spectra were recorded in the 4000−400 cm^{-1} spectral region at 8 K with a Nicolet SX60 FTIR spectrometer (1 cm^{-1} resolution) using up to 500 scans. Photolysis of the samples was performed at 8 K with a 193 nm eximer laser (MPB MSX-250, ∼15 mJ cm^{-2} pulse energy density) or by using the fourth harmonic of a Nd:YAG laser (Continuum Powerlite) at 266 nm. The number of laser pulses used for photolysis varied from 30 to 5000 and the repetition rate was 1 Hz (193 nm) and 10 Hz (266 nm). After photolysis, the samples were annealed at 40−70 K.

HBr/Xe. After deposition of a HBr/Xe (1:300−1000) matrix, the known absorptions of HBr monomer and HBr multimers are seen in IR spectra (see Figure 1).[20,21] The R branch of

* Corresponding author. E-mail: lignell@csc.fi. Fax: +358-9-19150279.
† University of Helsinki.
‡ University of Jyväskylä.

10.1021/jp801363u CCC: $40.75
Published on Web 05/27/2008

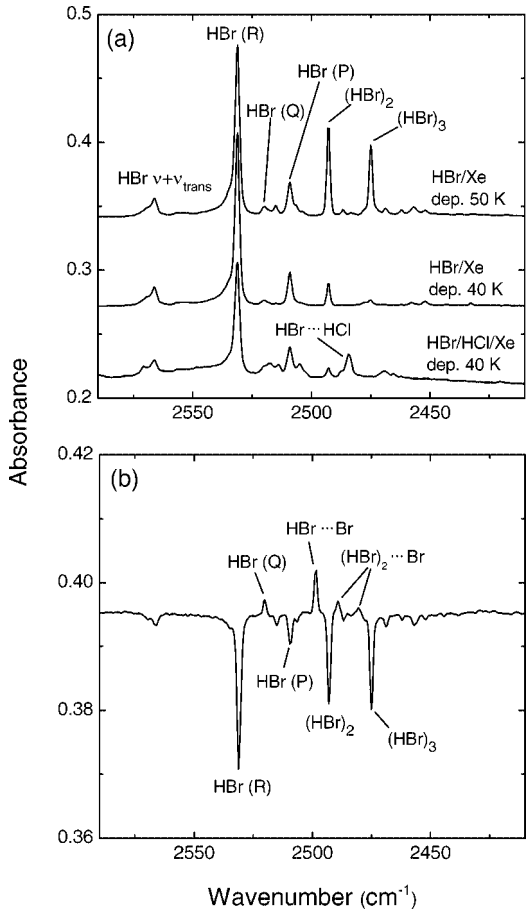

Figure 1. (a) FTIR spectra of the HBr/Xe (1:1000) and HBr/HCl/Xe (1:1:300) matrices measured at 8 K. The upper and middle traces show the effect of deposition temperature. The bands marked with P, Q, and R are due to the rotational structure of HBr monomer and the band marked with $\nu + \nu_{trans}$ is a vibrational band of HBr monomer coupled with a translational mode (see ref 22 for details). (b) FTIR spectra of HBr-related species after 193 nm photolysis (30 pulses, 14 mJ cm^{-2}) of a HBr/Xe sample. Photolysis of $(HBr)_2$ and $(HBr)_3$ leads to the formation of HBr···Br and $(HBr)_2$···Br complexes, respectively. The spectrum is a difference spectrum showing the results of photolysis.

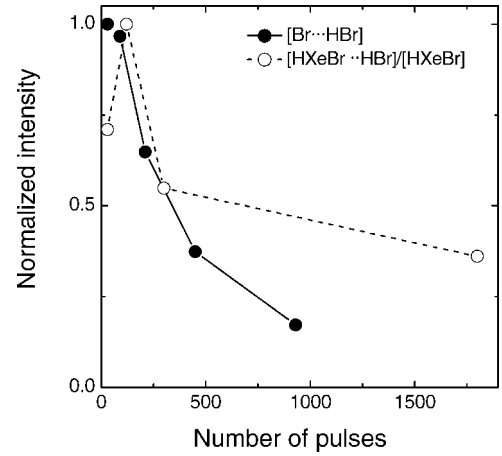

Figure 2. Formation of the HBr···Br complex during 193 nm photolysis of a HBr/Xe matrix (solid circles). The pulse energy density was 14 mJ cm^{-1}. Open circles present the (HXeBr···HBr)/HXeBr ratio calculated from the integrated absorptions. Deposition temperature was 50 K.

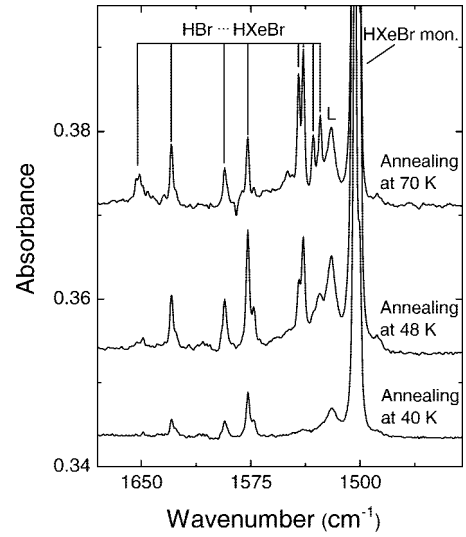

Figure 3. FTIR spectra of the HXeBr monomer and HXeBr···HBr complexes measured at 8 K. The HBr/Xe (1:1000) matrix was deposited at 50 K and irradiated by 120 pulses at 193 nm (12 mJ cm^{-2}). Annealing of a sample at 40 K leads to the diffusion of H atoms and formation of the HXeBr monomer and complexes. Annealing at higher temperatures modifies the HXeBr···HBr band structure. The band marked with L is a librational band of the HXeBr monomer (see ref. 28).

rotating HBr at 2531.1 cm^{-1} dominates and the Q (2520.0 cm^{-1}) and P branches (2508.9 cm^{-1}) are weaker. The vibrational band coupled with the translational mode is at 2566.3 cm^{-1}.[22] The deposition temperatures varied from 40 to 60 K, and the maximal amount of dimers was achieved for deposition at 50 K. At this temperature, the HBr dimer (2493.0 cm^{-1}) and trimer (2475.1 cm^{-1}) absorptions were ∼50% of the absorption intensity of the monomeric (R) band. A lower temperature deposition leads to more monomeric samples, and larger $(HBr)_n$ ($n \geq 3$) clusters are formed in samples deposited at higher temperatures. Complexes of HBr with N_2 and H_2O were not observed in any samples prepared.

Irradiation at 193 nm decomposes HBr. The HBr dimers and trimers are photodecomposed faster than the monomer: 13% of monomer and 34% of dimer absorptions were decomposed with 120 pulses (12 mJ cm^{-2}) at 193 nm radiation. Upon short photolysis, the Q branch of HBr was enhanced and new absorptions at 2498.3, 2489.2, and 2480.5 cm^{-1} appeared. These absorptions are due to the formation of the HBr···Br (2498.3 cm^{-1}) and $(HBr)_2$···Br (2489.2 and 2480.5 cm^{-1}) complexes (see Figure 1).[23] The HBr···Br concentration as a function of irradiation time is presented in Figure 2. The HBr···Br concentration is at a maximum after ∼30 pulses and decreases upon further photolysis, and after 300 pulses it is about two times lower than at the maximum.

As repeatedly demonstrated, UV photolysis of HX precursors produces H atoms in a xenon lattice.[24] Hydrogen atoms start diffusing in solid xenon upon annealing at ∼40 K.[25,26] The hydrogen mobility promotes a variety of solid-state chemical reactions including the formation of noble-gas hydrides.[8] In HBr/Xe matrices, we found the formation of HXeBr (H−Xe stretching absorption at 1503.7 cm^{-1}) and HXeH (1180.9 and 1166.2 cm^{-1}) molecules.[7,27] HXeBr also exhibits a librational band at 1519.6 cm^{-1}.[28] In matrices with a high HBr concentration, absorptions at 1577.0, 1592.9, 1629.1, and 1648.8 cm^{-1} are seen in the spectrum after annealing at 40 K, in addition to the HXeBr monomer bands (see Figure 3). Upon annealing at 48 K, a new absorption appears at 1538.9 cm^{-1} and the absorptions at 1577.0, 1592.9, 1629.1, and 1648.8 cm^{-1} increase. Annealing at 70 K enhances the 1648.8 cm^{-1} absorption and diminishes the absorption at 1577.0 cm^{-1}. In addition, the

TABLE 1: Monomer-to-Complex Blue-Shifts (in cm^{-1}) for the H−Xe Stretching Vibrations of the Experimentally Observed HXeY···HX (X, Y = Cl or Br) Complexes[a]

HXeBr···HBr	HXeBr···HCl	HXeCl···HCl
+23.6	+84.0	+30.1
+28.5	+92.1	+37.4
+35.3	+119.1	+50.2
+38.6	+121.5	+80.8
+73.3		+84.1
+89.1		+106.4
+125.9		+115.5
+148.9		
+245.4[b]		

[a] Experimental H−Xe stretching frequencies for HXeCl and HXeBr monomers are 1648.5 and 1503.7 cm^{-1}, respectively. [b] $HXeBr\cdots(HBr)_2$ trimer (tentative assignment).

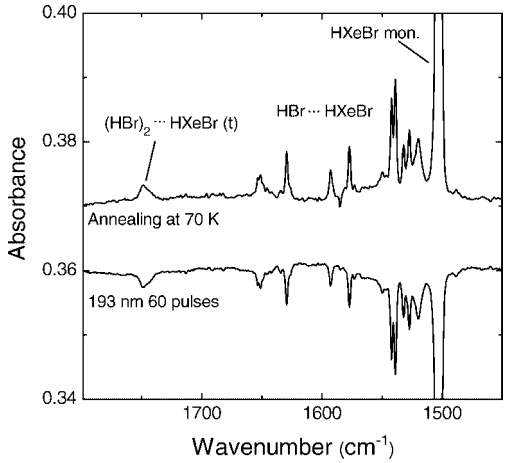

Figure 4. FTIR spectra of HXeBr monomer and complexes measured at 8 K. The HBr/Xe (1:1000) matrix was deposited at 50 K, irradiated by 120 pulses of 193 nm, and annealed at 70 K. The lower trace shows a result of photodecomposition of HXeBr and its complexes by 193 nm radiation (120 pulses, 12 mJ cm^{-2}).

absorption at 1538.9 cm^{-1} splits into four bands at 1527.3, 1532.2, 1538.9, and 1542.3 cm^{-1}. In more multimeric samples, an additional band at 1749.1 cm^{-1} rises after annealing at 48 K. We assign these new absorptions to the H−Xe stretching vibrations of a HXeBr molecule complexed with various HBr-related structures. The shifts of these absorptions from the HXeBr monomer band are presented in Table 1.

All the observed HXeBr-related bands are efficiently bleached by irradiating at 193 nm similarly to HXeBr monomer (see Figure 4). Upon this irradiation, the HBr···Br band at 2498.3 cm^{-1} increases. The second annealing of the sample at 60 K leads to the 35% recovery of the HXeBr monomer and complex absorptions.

HCl/Xe. The most efficient formation of HCl dimers was obtained by depositing a mixture of HCl/Xe (1:300) at 40 K. The absorptions of HCl (R) and HCl (P) at 2858.0 and 2837.7 cm^{-1} are seen in the spectra.[20,21] The bands of the HCl dimer at 2816.5 cm^{-1} and trimer at 2792.4 cm^{-1} were also found in agreement with literature (see Figure 5).[20,21]

Upon 193 nm photolysis, the HCl monomer and multimer bands decrease. Similarly to HBr, the decomposition of HCl multimers was faster compared to the monomer. After 600 pulses with a pulse energy density of 14 mJ cm^{-2}, the decomposition was 13% for HCl monomer and 24% for dimer. Upon irradiation, new bands appear at 2826.2 and 2794.8 cm^{-1}, which belong to the HCl···Cl and probably to $(HCl)_2$···Cl complex, respectively.[29] These bands are more difficult to assign

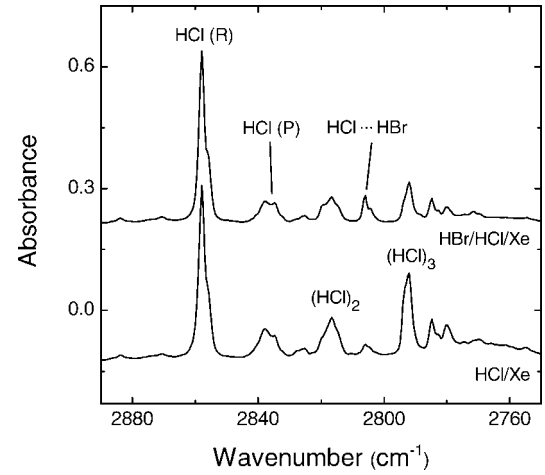

Figure 5. FTIR spectra of HCl/Xe (1:300) and HCl/HBr/Xe (1:1:300) matrices deposited at 40 K and measured at 8 K.

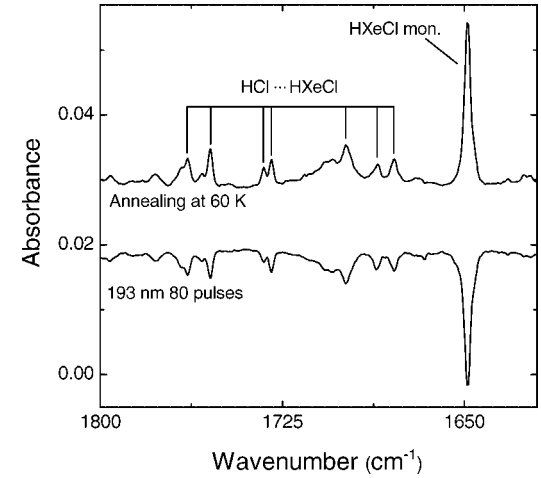

Figure 6. FTIR spectra of HXeCl monomer and HXeCl···HCl complexes measured at 8 K. The HCl/Xe (1:300) matrix was deposited at 40 K. The matrix was irradiated at 193 nm (600 pulses, 14 mJ cm^{-2}) and annealed at 60 K. The lower trace shows the result of photodecomposition of HXeCl and its complexes by 193 nm radiation.

than the corresponding HBr···Br bands due to their overlap with the HCl monomer and multimer bands.

Upon annealing at 40 K, the formation of HXeCl molecules (H−Xe stretching mode at 1648.5 cm^{-1}) is seen.[7] In addition to the HXeCl monomer band, new absorptions appear at 1699.4, 1729.8, 1754.6, and 1764.3 cm^{-1} in multimeric HCl/Xe samples (see Figure 6). The absorption at 1729.6 cm^{-1} is dominating, and the absorption at 1699.4 cm^{-1} is weak. Annealing at 48 K increases the 1699.4, 1754.6, and 1764.3 cm^{-1} bands. In addition, a new doublet at 1678.7 and 1685.7 cm^{-1} appears. Annealing at 60 K results in a minor change in the spectrum; the absorption bands become somewhat narrower probably due to thermal relaxation of the matrix environment. We assign these new bands to HXeCl complexed with HCl and the monomer-to-complex shifts of these bands are presented in Table 1. The HXeCl molecule efficiently decomposes under UV irradiation, and this can be used to identify the HXeCl···HCl absorptions. The lower trace in Figure 6 presents a result of photolysis by 193 nm, showing a decrease of all absorptions related to the HXeCl molecule in the H−Xe stretching region.

HBr/HCl/Xe. For the experiment with HBr/HCl/Xe matrices, we used two gas-phase sample bulbs with HCl/Xe (1:300) and HBr/Xe (1:300) mixtures. The deposition temperature of 40 K was used and the relative amounts of HCl and HBr were varied

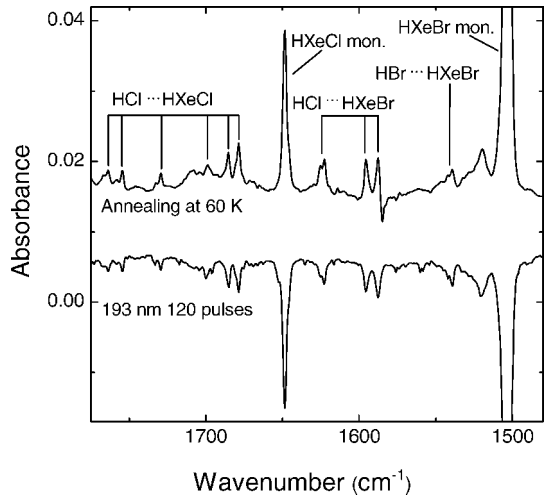

Figure 7. FTIR spectrum of HCl/HBr/Xe (1:1:300) matrix after photolysis and annealing the sample at 60 K (upper trace). The HXeCl, HXeCl···HCl, HXeBr, HXeBr···HBr, and HXeBr···HCl species are present in the experiments. The lower trace shows the decomposition of the species under 193 nm UV-radiation. Spectra are measured at 8 K.

by changing the gas flow rates. After deposition, monomer and multimer bands of both HCl and HBr are seen in the spectra. In addition, the HCl···HBr mixed complex bands are observed in the HCl and HBr stretching regions at 2805.9 and 2484.3 cm^{-1}, respectively.[30] Photolysis at 193 nm decomposed HBr and HCl monomers and multimers, HCl being more photostable than HBr. After 900 pulses at 193 nm (13 mJ cm^{-2}), HCl was decomposed by 21%, HBr by 66%, and the HCl···HBr complexes by ~37%. Upon photolysis, a probable HCl···Br band appeared at 2811.7 cm^{-1}.

Upon annealing at 40 K, both HXeCl and HXeBr form. The absorptions of HXeCl···HCl complexes described earlier also appear. In addition to the bands seen in HBr/Xe and HCl/Xe experiments, new absorptions are observed at 1587.6, 1595.8, and 1622.8 cm^{-1} (see Figure 7 and Table 1). We assign these bands to the HXeBr···HCl complexes. These bands increase upon further annealing at 48 and 60 K. After annealing at 48 K, a weak absorption belonging to the HXeBr···HBr complex appears at 1538.9 cm^{-1}. Short irradiation at 193 nm (120 pulses with 13 mJ cm^{-2}) bleaches completely the absorptions of HXeCl, HXeBr, and their hydrogen halide complexes (see the lower trace in Figure 7).

Computations

The equilibrium structures and harmonic vibrational spectra were computed at the full MP2 level of theory, i.e., explicitly correlating all included electrons during the calculations. Two different basis set combinations were used. The first basis set (basis 1) contains the standard split-valence basis set augmented with diffusion functions [6-311++G(2d,2p)] for hydrogen and chlorine atoms. Here the xenon and bromine atoms were described by a valence basis picturing 18 and 17 valence electrons, respectively, in connection with effective core potentials (ECP) developed by LaJohn and co-workers.[31] Such basis sets have been previously used for calculations of geometry and absorption spectra of noble-gas hydrids to aid experimental work.[8,32,33] The second basis set used in the present study (basis 2) is more flexible compared to basis 1. The second basis set employs the aug-cc-pVTZ basis for the hydrogen atom and the cc-pVTZ basis set for chlorine. Bromine and xenon are

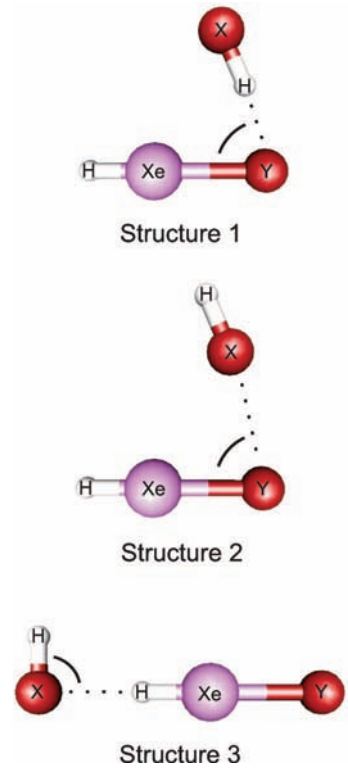

Figure 8. Computational minimum-energy structures of the HXeY···HX (X, Y = Cl and Br) complexes. Structural parameters at different levels of computation are given in Table 2.

described with the cc-pVTZ-PP valence basis sets combined with small-core Stuttgart ECPs.[34] These basis sets retain 25 and 26 electrons in the valence space of Br and Xe atoms, respectively, and they were retrieved from the EMSL basis set database.[35]

The interaction energies of the complexes were estimated as the difference of the total energy between the complex and the monomers where the subunit wave functions were derived in the dimer centered basis set (DCBS). This approach corresponds to the counterpoise correction proposed by Boys and Bernardi,[36] aimed at the minimization of the basis set superposition error (BSSE) in the interaction energy. The charge distributions were calculated by using natural population analysis (NPA). All calculations were performed with the GAUSSIAN 03 program[37] on the Sun Fire 25K computer at the CSC, Center for Scientific Computing (Espoo, Finland).

The intermolecular potential energy surfaces of HXeY···HX (X, Y = Cl and Br) complexes were preliminary scanned with basis 1. These calculations revealed three stable complex structures. In two of the structures, the HY molecule forms a bent structure close to the halogen end of the HXeY molecule (see Figure 8). The third complex structure is formed by interaction between the hydrogen of the HXeY and the HX molecule. The halogen atom of the HX subunit is on the axis of HXeY whereas the hydrogen is tilted by ~90° to this axis. Reoptimizations of these three local minima structures using the larger basis set still maintained the preliminary obtained complex structures but decreasing the H−Xe (0.01−0.03 Å) and Xe−Y (0.02−0.07 Å) bond distances in the HXeY subunits.

The computed structural parameters of the HXeY···HX complexes are presented in Table 2. Most of the complex structures are very similar for basis 1 and basis 2. The most significant differences appear in the structure of the HXeY molecules. As concerns the complex structures, a rather large

TABLE 2: Computed Equilibrium Structures of the HXeY···HX (X, Y = Cl and Br) Complexes[a]

	r(H−Xe)	r(Xe−Y)	r(X/Y···H)	r(H−X)	r(Y···X)	∠(XeY···H)/∠(Xe−H···X)	∠(Xe−Y···X)	∠(H/Y···X−H)
				HXeBr Monomer				
basis 1[b]	1.717	2.908						
basis 2[c]	1.688	2.744						
				HXeCl Monomer				
basis 1	1.685	2.662						
basis 2	1.673	2.593						
				HXeBr···HBr				
structure 1/basis 1	1.687	2.940	2.488	1.394		79.5		165.1
structure 1/basis 2	1.661	2.970	2.200	1.436		76.2		179.4
structure 2/basis 1	1.711	2.914		1.380	3.891		75.8	169.5
structure 2/basis 2	1.681	2.755		1.402	3.524		75.3	170.5
structure 3/basis 1	1.705	2.923	2.889	1.379		175.1		86.7
structure 3/basis 2	1.683	2.773	2.556	1.401		179.8		91.1
				HXeBr···HCl				
structure 1/basis 1	1.655	2.996	1.870	1.379		75.4		172.0
structure 1/basis 2	1.662	2.797	2.213	1.305		76.3		168.1
structure 2/basis 1	1.709	2.912		1.271	3.768		70.1	173.0
structure 2/basis 2	1.685	2.748		1.273	3.606		72.0	170.8
structure 3/basis 1	1.703	2.920	2.796	1.271		172.6		107.9
structure 3/basis 2	1.680	2.766	2.573	1.273		179.6		99.3
				HXeCl···HBr				
structure 1/basis 1	1.667	2.700	2.266	1.397		87.3		165.0
structure 1/basis 2	1.648	2.656	2.049	1.439		80.3		169.9
structure 2/basis 1	1.682	2.667		1.380	3.659		82.7	169.4
structure 2/basis 2	1.667	2.605		1.402	3.399		79.5	170.3
structure 3/basis 1	1.678	2.685	2.880	1.379		178.0		89.3
structure 3/basis 2	1.669	2.621	2.569	1.401		179.1		92.6
				HXeCl···HCl				
structure 1/basis 1	1.658	2.727	2.073	1.309		83.6		165.6
structure 1/basis 2	1.648	2.655	2.059	1.308		80.3		167.9
structure 2/basis 1	1.683	2.666		1.272	3.559		76.1	171.0
structure 2/basis 2	1.670	2.598		1.272	3.503		75.8	169.8
structure 3/basis 1	1.677	2.682	2.784	1.271		177.2		108.1
structure 3/basis 2	1.667	2.615	2.573	1.273		179.9		99.6

[a] The bond lengths are in Ångströms and angles in degrees. [b] Basis 1: MP2(full)/6-311++G(2d,2p),[H,Cl], LJ18[Xe,Br]. [c] Basis 2: MP2(full)/aug-cc-pVTZ[H], cc-pVTZ[Cl], cc-pVTZ-PP[Xe,Br].

discrepancy between the two computational levels takes place for structure 1 of the HXeBr···HCl complex, and this should be commented. The smaller computational level (basis 1) produces a very small intermolecular distance between the complex subunits (1.87 Å). Such a short distance between the subunits is accompanied by a large intramolecular reorganization (Table 2) and charge redistribution (Table 3). The computed partial charges for the atoms of the HCl molecule are twice as large as compared to the monomer. Additionally, the two halogen atoms have almost equal partial charges, which suggests the formation of an ion-pair type of structure where $(XeH)^+$ is in close contact with bihalide anion $(BrHCl)^-$. This situation is probably due to the computational approach used where the description of the atomic electron clouds are not in balance and a more flexible basis on chlorine results in a basis set borrowing from the bromine atom of the HXeBr molecule. The basis set superposition error in this case is probably large enough to divert this complex structure from the other HXeY···HX complexes and the results obtained for HXeBr···HCl with the larger basis set (basis 2). Basis 2 is supposed to be more balanced because all the atomic basis sets are of about the same quality. Basis 2 leads to the HXeBr···HCl intermolecular distance of 2.213 Å, which is similar to all other complexes in this study. The computed partial charges with basis 2 are close to the values obtained for unperturbed molecules. These results on HXeBr···HBr complex with basis 2 suggest that only small structural and electronical perturbations are induced by complexation.

The BSSE-corrected intermolecular interaction energies of various complexes are presented in Table 4. Structure 1 is the most strongly bound complex. For all four molecular combinations the BSSE-corrected interaction energies are estimated to be close to -2500 cm^{-1} (-30 kJ mol^{-1}) at the MP2/basis 2 level of theory. These interaction energies are about 5 times larger than those of structures 2 and 3 and of the corresponding $(HCl)_2$ and $(HBr)_2$ dimers.[30] We believe that this is not only an effect of favorably dipole−dipole arrangement but due to the increased delocalized electron density giving the complex a stabilizing effect from the $(HXe^+\cdots YHX^-)$ structure. The two other complex structures represent a more usual dipole−dipole interaction. Structures 1 and 3 exhibit hydrogen bonding between the complex partners whereas structure 2 forms a van der Waals complex. The larger and more balanced approach using basis 2 yields larger interaction energies (E_{int}) for the complexes than smaller basis 1. The result can differ more than by a factor of 2 between the two computational levels used here. This indicates that it is uncertain to rely on basis 1 as the only computational method for complexes of HXeY molecules.

Table 5 presents the computed vibrational shifts of the H−Xe and H−X stretching modes for computationally studied complexes. The full vibrational spectra computed for all complex structures are presented in Tables S1 and S2 of the Supporting Information. All HXeY···HX complex structures obtained in the present work have only real vibrational frequencies, which indicate true local minima on the potential energy surfaces. For

TABLE 3: Computed Natural Charges of the HXeY···HY (X, Y = Cl and Br)

	HXeY			HX	
	q(H)	*q*(Xe)	*q*(Y)	*q*(H)	*q*(X)
		HXeBr/HBr Monomer			
basis 1	−0.066	0.666	−0.600	0.120	−0.120
basis 2	−0.033	0.655	−0.622	0.185	−0.185
		HXeCl/HCl Monomer			
basis 1	−0.053	0.747	−0.694	0.251	−0.251
basis 2	−0.028	0.694	−0.666	0.253	−0.253
		HXeBr···HBr			
structure 1/basis 1	−0.027	0.697	−0.619	0.144	−0.194
structure 1/basis 2	0.016	0.679	−0.589	0.176	−0.281
structure 2/basis 1	−0.060	0.673	−0.608	0.111	−0.116
structure 2/basis 2	−0.022	0.662	−0.627	0.169	−0.181
structure 3/basis 1	−0.051	0.670	−0.639	0.131	−0.111
structure 3/basis 2	−0.014	0.644	−0.669	0.196	−0.157
		HXeBr···HCl			
structure 1/basis 1	0.023	0.734	−0.525	0.200	−0.431
structure 1/basis 2	0.015	0.679	−0.605	0.252	−0.341
structure 2/basis 1	−0.059	0.677	−0.608	0.240	−0.250
structure 2/basis 2	−0.029	0.659	−0.625	0.245	−0.250
structure 3/basis 1	−0.046	0.673	−0.637	0.259	−0.249
structure 3/basis 2	−0.009	0.649	−0.662	0.264	−0.242
		HXeCl···HBr			
structure 1/basis 1	−0.020	0.762	−0.693	0.153	−0.201
structure 1/basis 2	0.024	0.714	−0.634	0.187	−0.291
structure 2/basis 1	−0.050	0.751	−0.697	0.109	−0.113
structure 2/basis 2	−0.018	0.700	−0.671	0.167	−0.178
structure 3/basis 1	−0.038	0.742	−0.723	0.132	−0.113
structure 3/basis 2	−0.011	0.679	−0.704	0.197	−0.161
		HXeCl···HCl			
structure 1/basis 1	−0.004	0.769	−0.680	0.265	−0.351
structure 1/basis 2	0.023	0.714	−0.647	0.259	−0.349
structure 2/basis 1	−0.051	0.751	−0.695	0.239	−0.244
structure 2/basis 2	−0.025	0.698	−0.669	0.243	−0.248
structure 3/basis 1	−0.034	0.745	−0.721	0.260	−0.250
structure 3/basis 2	−0.007	0.685	−0.699	0.264	−0.244

TABLE 4: BSSE-Corrected Interaction Energies (in cm^{-1}) of the HXeY···HX (X, Y = Cl and Br) Complexes

	structure 1	structure 2	structure 3
		HBr···HXeBr	
basis 1	−1100	−208	−134
basis 2	−2384	−792	−490
		HCl···HXeCl	
basis 1	−2754	−356	−394
basis 2	−2838	−488	−460
		HCl···HXeBr	
basis 1	−1875	−161	−300
basis 2	−2534	−471	−472
		HBr···HXeCl	
basis 1	−1540	−323	−224
basis 2	−2638	−799	−501

structure 1, the complexation-induced blue-shifts of the H−Xe stretching mode are the largest (typically >100 cm^{-1}) and the values obtained with the two basis sets used are similar. Structures 2 and 3 have smaller blue-shifts, from 10 to 90 cm^{-1} depending on the system and the computational level. Basis 2 gives larger blue-shifts (∼40 cm^{-1}) for the structure 3 in the HXeBr···HCl and HXeCl···HCl complexes and smaller blue-shifts (∼10−20 cm^{1}) in the HXeBr···HBr and HXeCl···HBr systems than basis 1. The ν(H−Xe) blue-shifts are attributed to the charge redistribution in the HXeY molecules upon complexation enhancing its (HXe)$^{+}$Y^{-} ion-pair character.[9,10] This charge redistribution correlates with shortening of H−Xe bond length, blue-shift of its vibrational frequency, and decrease of its absorption intensity.

In addition to the HXeY···HX dimers, we studied minimum energy structures of the HXeBr···(HBr)$_2$ trimer at the MP2/basis 2 level of theory. We concentrated only on the structure shown in Figure 9. This structure was chosen because this geometry consists of the strongest HXeBr···HBr complex arrangement (structure 1) and the global minimum of a HBr dimer.[30] The computational monomer-to-complex shift of H−Xe stretching vibration for the trimer is 251.7 cm^{-1}. Its BSSE-corrected interaction energy is −4580 cm^{-1} (−55 kJ mol^{-1}).

Discussion

The assignment of the HXeY···HX complexes is based on the following arguments. By changing the HY/Xe concentration and deposition temperature, the relative amounts of hydrogen halide multimers can be changed. Higher deposition temperatures and larger HY/Xe (Y = Cl, Br) ratios lead to more multimeric matrices (see Figure 1). It is clear that the HXeY···HX complexes are produced from the HY···HX complexes. Indeed, the bands assigned to HXeY···HX complexes correlate with the HY···HX dimers in the deposited matrices. The matrices with smaller amounts of HY···HX dimers yield weaker HXeY···HX complex bands. The HX···Y intermediates obtained from photodecomposition of the HY···HX dimers are the direct precursors for the HXeY···HX complexes. The HBr···Br concentration as a function of irradiation time

TABLE 5: Computational Monomer-to-Complex Shifts (in cm^{-1}) of the HXeY···HX (X, Y = Cl and Br) Complexes[a]

	monomer	structure 1	stucture 2	structure 3
		HBr···HXeBr		
		ν(H−Xe)		
basis 1	1679.1 (4102)	+140.2 (3131)	+24.7 (3883)	+78.4 (2329)
basis 2	1818.3 (1734)	+119.1 (1193)	+26.5 (1552)	+17.7 (350)
		ν(H−Br)		
basis 1	2854.0 (5)	−212.7 (526)	−12.9 (1)	−3.6 (12)
basis 2	2780.1 (13)	−471.4 (2309)	−30.0 (1)	−20.2 (28)
		HCl···HXeCl		
		ν(H−Xe)		
basis 1	1903.8 (1733)	+126.2 (1085)	+8.7 (1630)	+48.8 (985)
basis 2	1920.1 (1144)	+116.7 (733)	+9.9 (1076)	+35.6 (352)
		ν(H−Cl)		
basis 1	2998.1 (52)	−536.8 (1481)	−15.1 (30)	−15.1 (74)
basis 2	3057.6 (46)	−506.9 (1253)	−14.8 (29)	−19.6 (67)
		HCl···HXeBr		
		ν(H−Xe)		
basis 1	1679.1 (4102)	+348.6 (1692)	+31.7 (3812)	+91.1 (2698)
basis 2	1818.3 (1734)	+122.1 (1201)	+10.9 (1638)	+47.8 (633)
		ν(H−Cl)		
basis 1	2998.1 (52)	−1364.6 (4191)	−13.0 (30)	−13.9 (78)
basis 2	3057.6 (46)	−466.0 (1205)	−16.1 (28)	−19.9 (69)
		HBr···HXeCl		
		ν(H−Xe)		
basis 1	1903.8 (1733)	+85.6 (1287)	+11.6 (1638)	+40.9 (800)
basis 2	1920.1 (1144)	+112.4 (764)	+23.7 (1013)	+8.8 (181)
		ν(H−Br)		
basis 1	2854.0 (5)	−240.0 (612)	−13.9 (1)	−4.4 (11)
basis 2	2780.1 (13)	−507.8 (1312)	−26.1 (1)	−18.0 (26)

[a] The infrared absorption intensities are marked in parentheses (km mol^{-1}). The complex structures are shown in Figure 9.

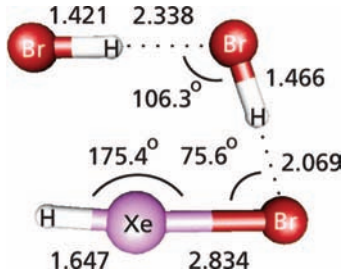

Figure 9. Computational structure of the HXeBr···(HBr)$_2$ trimer. The bond lengths are in Å and angles in degrees.

is presented in Figure 2 (solid circles) and the (HXeBr···HBr)/HXeBr ratio achieved by annealing (open circles) follows this precursor concentration. After very long photolysis (>4000 pulses, ~15 mJ cm^{-1}), the formation of the HXeY···HX complexes was inefficient.

The double precursor (HCl/HBr/Xe) experiments show new HXeBr···HCl complex bands in the HXeBr spectral region. HCl is much more photostable than HBr under 193 nm radiation. Thus, the Br···HCl formation is a dominating channel in the photolysis of the HBr···HCl dimer, which allows efficient formation of the HXeBr···HCl complex. In the matrices with both (HBr)$_2$ and HBr···HCl dimers, longer photolysis leads mainly to the Br···HCl intermediates as compared to Br···HBr and hence to the more efficient formation of HXeBr···HCl as compared to HXeBr···HBr (see Figure 7). The same reasoning corroborates the negligible formation of HXeCl···HBr compared to HXeCl···HCl.

The HNgY molecules are known to decompose efficiently under UV light.[38] Figures 4, 6, and 7 show bleaching of the bands related to HXeBr and HXeCl species obtained by 60−120 pulses of 193 nm radiation. The HBr···Br complex is formed upon short UV photolysis of HXeBr···HBr complex. During this photolysis, decomposition of (HBr)$_2$ is minor, and it does not contribute significantly to the HBr···Br complex formation. This observation indicates that HBr···Br is formed from the decomposition of HXeBr···HBr complexes. Similarly, Cl···HCl was formed after UV photolysis of HXeCl···HCl; however, no Br···HCl was observed when the HXeBr···HCl complex was decomposed.

The experimental and computational vibrational frequencies should be compared. Computationally, we found three structures for the HXeY···HX (X, Y = Cl and Br) complexes (see Figure 8 and Table 4). The only experimentally observed absorption of HXeY (Y = Cl and Br) is the H−Xe stretching vibration and the experimental and computational data for this mode are in good qualitative agreement (see Tables 1 and 5). The computations and experiments give blue-shifts for the H−Xe stretching vibrations of HXeY upon complexation with HX. Experimentally, the HXeBr···HBr complexes are found in three sets of blue-shifted absorptions: 24−39 cm^{-1}, 73−89 cm^{-1}, and 126−145 cm^{-1} (see Figure 3). The two sets with larger shifts are suitable for structure 1 (computational shift +119 cm^{-1}). The bands with lower blue-shifts (24−39 cm^{-1}) could be connected with structures 2 and 3 (computational shifts +27 and +18 cm^{-1}, respectively). According to the computations, structure 2 has the largest absorption intensity, by a factor of 4 larger than structure 3. In the experiments, the doublet band with shifts of +35 and +37 cm^{-1} are the most intense and they most likely belong to structure 2. The HXeCl···HCl complexes (see Figure 6) show similar absorptions to the HXeBr···HBr complexes, and similar assignments of the experimental absorptions are plausible. The HXeCl···HCl complex bands blue-shifted by 30−50 cm^{-1} can be assigned to structures 2 and 3 with computational shifts of +10 and +36 cm^{-1}, respectively. The bands shifted by 80−84 and 106−115 cm^{-1} are presumably due to structure 1 with the computational shift of +117 cm^{-1}. The bands shifted by 80−84 cm^{-1} probably belong to a distorted geometry of structure 1. The only experimentally observed "mixed" complex is HXeBr···HCl and has blue-shifts of 80−120 cm^{-1} (see Figure 7) that are probably related to structure 1 (computational shift +122 cm^{-1}).

The interaction energies of structure 1 are about 5 times larger than those of structures 2 and 3, suggesting that it should form more efficiently. At lower annealing temperature, the intensity of absorptions assigned to structure 1 are comparable to other complex absorptions in the spectra. This means that the complexes after photolysis and annealing are not in thermodynamic equilibrium according to the calculated interaction energies. A reason for this difference is the surrounding xenon matrix that influences the formation of the complexes. As presented in Figure 3, the complex bands are changed by annealing temperature. Annealing at higher temperatures (70 K) leads to new complex bands at the lower shifting region (+24 and +29 cm^{-1}) and to modification of bands shifted by +35 and +37 cm^{-1}. We may connect this behavior to the thermal relaxation of the surrounding matrix producing some changes of structures 2 and 3. The absorptions shifted by +149 and +126 cm^{-1} increase and absorptions shifted by +73 and +89 cm^{-1} decrease upon annealing at 70 K, indicating transformation of structure 1 to more stable configurations. Conversion of structures 2 and 3 to structure 1 does not take place most probably due to the large energy barriers between these structures in solid xenon.

According to the computations, the HX stretching absorption intensity of structures 1 should be largely activated upon complexation. However, no conclusive assignment of this absorption is done. The most probable reasons for this are the following. A strong enhancement of this vibration intensity occurs only in structure 1, and HX in structures 2 and 3 has absorption intensities similar to the HX monomer. A small change from the geometry of structure 1 is likely to decrease this intensity. In a matrix, the complex structures are distorted, which can limit the increase of HX vibrational intensity upon complexation. In addition, it is possible that calculations overestimate the H−X stretching intensity and that experimental absorptions are split and/or broadened making their observation difficult.

It should be emphasized that the assignments of the experimental H−Xe stretching bands to the computational structures are somewhat uncertain due to following reasons. The computational structures refer to the gas phase whereas the experiments are done in solid xenon. The complexes are formed in a matrix cage that is not optimal to accommodate them. The HXeY molecules probably have large vibrational shifts in noble-gas matrices (solvation effect) from the gas-phase values.[23,39] When making structural assignment, it should be taken into account that the HXeY monomers are "complexed" with the surrounding matrix atoms. Several attempts to simulate the effect of surrounding matrix on the vibrational properties of HNgY molecules have been done;[40–42] however, the task becomes much more complicated for the HNgY complexes, and this exceeds the framework of the present study.

In addition to the bands assigned to the HXeBr···HBr dimers, we found an annealing-induced absorption at 1749 cm^{-1}, i.e., blue-shifted by 245 cm^{-1} from the HXeBr monomer band (see Figure 4). We tentatively assigned this band to the HXeBr···$(HBr)_2$ trimer. The computational complexation-induced shift of the HXeBr···$(HBr)_2$ trimer (see Figure 9) is +252 cm^{-1}, which is close to the experimental value. This band was strongest in the experiments with higher HBr multimer concentration supporting its formation from $(HBr)_3$ trimer via the Br···$(HBr)_2$ intermediate. Similarly, the HXeOH···$(H_2O)_2$ trimer was found to have an increased blue-shift compared to the HXeOH···H_2O dimer (+164 vs +103 cm^{-1}), supporting our assignment of the ternary HXeBr···$(HBr)_2$ complex.[12] This would be a record-breaking value for a complexation-induced blue-shift.

The presence of HXeY impurity complexes (e.g., with N_2 and O_2) can be ruled out, because our experimental spectra did not show any presence of impurity-induced species (e.g., HOO from O_2 + H reaction). We performed experiments with HBr/N_2/Xe matrices and no additional bands in the HXeBr region were found. The formation of a hypothetical Br···HXeBr complex is also improbable due to the high reactivity of a bromine atom.

Previously, McDowell and Yen et al. reported computational results on HNgF···HF (Ng = Ar, Kr, and Xe) complexes.[18,19] Their results are relevant to our present study because they give an example of complexes between noble-gas hydride and hydrogen halide molecules. Their studies showed two minimum energy structures for the studied complexes, and these geometries are similar to structures 1 and 3 obtained in the present study. They reported large computational blue-shifts of the H−Ng stretching vibrations (up to ∼400 cm^{-1}), and the interaction energies of their complexes are comparable to our present systems. They also suggested a strong increase of intensity of the HF vibration absorption upon complexation. No experimental research is done on those interesting complexes.

Conclusions

In the present work, we studied experimentally and computationally the HXeY···HX (X, Y = Cl and Br) complexes. These complexes were prepared by photolyzing the HX···HY (X, Y = Cl and Br) dimers to the Y···HX radical complexes and by subsequent annealing-induced mobilization of H atoms in solid xenon. Computationally, we found three structures for HXeY···HX (X, Y = Cl and Br) complexes and their predicted counterpoise-corrected interaction energies varied between −460 and −2800 cm^{-1}. From experiments three such complexes could be assigned: HXeBr···HBr, HXeBr···HCl, and HXeCl···HCl. The negligible formation of HXeCl···HBr complex can be explained by the lower photostability of HBr compared to HCl in HCl/HBr/Xe matrices. We also found one experimental absorption possibly belonging to the HXeBr···$(HBr)_2$ trimer, and the vibrational shift (+245 cm^{-1}) observed for this species agrees with our computational model system forming a cyclic ternary complex (+252 cm^{-1}).

The experimental assignment was done using the intense H−Xe stretching absorption. The computations suggest large blue-shifts for this vibrational frequency upon complexation and we observed comparable blue-shifted absorptions in experiments. The experimentally obtained blue-shifts upon complexation are 24−149 cm^{-1} for HXeBr···HBr, 84−122 cm^{-1} for HXeBr···HCl, and 30−116 cm^{-1} for HXeCl···HCl. The corresponding computational estimates (MP2/basis 2) for the blue-shifts are 18− 119 cm^{-1} (HXeBr···HBr), 11−122 cm^{-1} (HXeBr···HCl), 10−117 cm^{-1} (HXeCl···HCl), and 9−112 cm^{-1} (HXeCl···HBr) depending on the complex structure. We tentatively assign the blue-shifts >70 cm^{-1} to structure 1 and the blue-shifts <70 cm^{-1} to structures 2 and 3 (see Figure 8) of HNgY···HX complexes. The splitting of experimental absorptions is attributed to multiple matrix sites of complexes in solid xenon.

Acknowledgment. The Academy of Finland supported this research, and the research done in Helsinki was performed within the Finnish Center of Excellence "Computational Molecular Science" (2006−2011). The CSC, Center for Scientific Computing Ltd. (Espoo, Finland), is thanked for providing computer facilities.

Supporting Information Available: Tables of vibrational frequencies and IR absorption intensities. This material is available free of charge via the Internet at http://pubs.acs.org.

References and Notes

(1) Pimentel, G. C.; McLellan, A. L. *The Hydrogen Bond*; W. H. Freeman and Co.: San Francisco, 1960.
(2) Badger, R. M.; Bauer, S. H. *J. Chem. Phys.* **1937**, *5*, 839.
(3) Hobza, P.; Havlas, Z. *Chem. Rev.* **2000**, *100*, 4253.
(4) Barnes, A. J. *J. Mol. Struct.* **2004**, *704*, 3.
(5) Kryachko, E. S. in *Hydrogen Bonding - New Insights*; Grabowski, S. J., Ed.; Springer: Dordrecht, The Netherlands, 2006; Chapter 8.
(6) Joseph, J.; Jemmis, E. D. *J. Am. Chem. Soc.* **2007**, *129*, 4620, and references therein.
(7) Pettersson, M.; Lundell, J.; Räsänen, M. *J. Chem. Phys.* **1995**, *102*, 6423.
(8) Pettersson, M; Khriachtchev, L.; Lundell, J.; Räsänen, M. In *Inorganic Chemistry in Focus II*; Meyer, G., Naumann, D., Wesemann, L., Eds.; Wiley-VCH: Weinheim, 2005; pp 15−34.
(9) Lignell, A; Khriachtchev, L.; Pettersson, M.; Räsänen, M. *J. Chem. Phys.* **2002**, *117*, 961.
(10) Lignell, A; Khriachtchev, L.; Pettersson, M.; Räsänen, M. *J. Chem. Phys.* **2003**, *118*, 11120.

(11) Tanskanen, H.; Johansson, S.; Lignell, A; Khriachtchev, L.; Räsänen, M. *J. Chem. Phys.* **2007**, *127*, 154313.
(12) Nemukhin, A. V.; Grigorenko, B. L.; Khriachtchev, L.; Tanskanen, H.; Pettersson, M; Räsänen, M. *J. Am. Chem. Soc*. **2002**, *124*, 10706.
(13) Lignell, A; Khriachtchev, L.; Pettersson, M.; Räsänen, M. *Chem. Phys. Lett.* **2004**, *390*, 256.
(14) Lundell, J.; Berski, S.; Lignell, A.; Latajka, Z. *J. Mol. Struct.* **2006**, *790*, 31.
(15) McDowell, S. A. C. *Chem. Phys.* **2006**, *328*, 69.
(16) McDowell, S. A. C. *J. Chem. Phys.* **2005**, *122*, 204309.
(17) McDowell, S. A. C. *Chem. Phys. Lett.* **2005**, *406*, 228.
(18) McDowell, S. A. C. *Chem. Phys. Lett.* **2003**, *377*, 143.
(19) Yen, S.-Y.; Mou, C.-H.; Hu, W.-P. *Chem. Phys. Lett.* **2004**, *383*, 606.
(20) Mann, D. E.; Acquista, N.; White, D. *J. Chem. Phys.* **1966**, *44*, 3453.
(21) Bowers, M. T.; Flygare, W. H. *J. Chem. Phys.* **1966**, *44*, 1389.
(22) Hallam, H. E. In *Vibrational Spectroscopy of Trapped Species*, Hallam, H. E., Ed.; John Wiley & Sons: Bristol, U.K., 1973; Chapter 3.
(23) Lorenz, M.; Kraus, D.; Räsänen, M.; Bondybey, V. E. *J. Chem. Phys.* **2000**, *112*, 3803.
(24) Khriachtchev, L.; Pettersson, M.; Räsänen, M. *Chem. Phys. Lett.* **1998**, *288*, 727.
(25) Eberlein, J.; Creutzburg, M. *J. Chem. Phys.* **1997**, *106*, 2188.
(26) Khriachtchev, L.; Tanskanen, H.; Pettersson, M.; Räsänen, M.; Feldman, V.; Sukhov, F.; Orlov, A.; Shestakov, A. F. *J. Chem. Phys.* **2002**, *116*, 5708.
(27) Pettersson, M.; Lundell, J.; Räsänen, M. *J. Chem. Phys.* **1995**, *103*, 205.
(28) Khriachtchev, L.; Lignell, A.; Juselius, J.; Räsänen, M.; Savchenko, E. *J. Chem. Phys.* **2005**, *122*, 014510.
(29) Liu, K.; Kolesov, A.; Partin, J. W.; Bezel, I.; Wittig, C. *Chem. Phys. Lett.* **1999**, *299*, 374.
(30) Latajka, Z.; Scheiner, S. *Chem. Phys.* **1997**, *216*, 37.
(31) LaJohn, L. A.; Christiansen, P. A.; Ross, R. B.; Atashroo, T.; Ermler, W. C. *J. Chem. Phys.* **1987**, *87*, 2812.
(32) Pettersson, M.; Lundell, J.; Räsänen, M. *Eur. J. Inorg. Chem.* **1999**, 729.
(33) Lundell, J.; Chaban, G. M.; Gerber, R. B. *J.Phys. Chem. A* **2000**, *104*, 7944.
(34) Peterson, K. A.; Figgen, D.; Goll, E.; Stoll, H.; Dolg, M. *J. Chem. Phys.* **2003**, *119*, 11113.
(35) Basis sets were obtained from the Extensible Computational Chemistry Environment Basis Set Database, Version 02/02/06, as developed and distributed by the Molecular Science Computing Facility, Environmental and Molecular Sciences Laboratory, which is part of the Pacific Northwest Laboratory, P.O. Box 999, Richland, WA 99352, U.S.A., and funded by the U.S. Department of Energy. The Pacific Northwest Laboratory is a multiprogram laboratory operated by Battelle Memorial Institute for the U.S. Department of Energy under contract DE-AC06−76RLO 1830. Contact Karen Schuchardt for further information.
(36) Boys, S. F.; Bernardi, F. *Mol. Phys.* **1970**, *19*, 553.
(37) Frisch, M. J.; Trucks, G. W.; Schlegel, H. B.; Scuseria, G. E.; Robb, M. A.; Cheeseman, J. R.; Montgomery, J. A., Jr.; Vreven, T.; Kudin, K. N.; Burant, J. C.; Millam, J. M.; Iyengar, S. S.; Tomasi, J.; Barone, V.; Mennucci, B.; Cossi, M.; Scalmani, G.; Rega, N.; Petersson, G. A.; Nakatsuji, H.; Hada, M.; Ehara, M.; Toyota, K.; Fukuda, R.; Hasegawa, J.; Ishida, M.; Nakajima, T.; Honda, Y.; Kitao, O.; Nakai, H.; Klene, M.; Li, X.; Knox, J. E.; Hratchian, H. P.; Cross, J. B.; Bakken, V.; Adamo, C.; Jaramillo, J.; Gomperts, R.; Stratmann, R. E.; Yazyev, O.; Austin, A. J.; Cammi, R.; Pomelli, C.; Ochterski, J. W.; Ayala, P. Y.; Morokuma, K.; Voth, G. A.; Salvador, P.; Dannenberg, J. J.; Zakrzewski, V. G.; Dapprich, S.; Daniels, A. D.; Strain, M. C.; Farkas, O.; Malick, D. K.; Rabuck, A. D.; Raghavachari, K.; Foresman, J. B.; Ortiz, J. V.; Cui, Q.; Baboul, A. G.; Clifford, S.; Cioslowski, J.; Stefanov, B. B.; Liu, G.; Liashenko, A.; Piskorz, P.; Komaromi, I.; Martin, R. L.; Fox, D. J.; Keith, T.; Al-Laham, M. A.; Peng, C. Y.; Nanayakkara, A.; Challacombe, M.; Gill, P. M. W.; Johnson, B.; Chen, W.; Wong, M. W.; Gonzalez, C.; Pople, J. A. *Gaussian 03*, revision C.02; Gaussian, Inc.: Wallingford, CT, 2004.
(38) Ahokas, J.; Kunttu, H.; Khriachtchev, L.; Pettersson, M.; Räsänen, M. *J. Phys. Chem. A* **2002**, *106*, 7743.
(39) Tanskanen, H.; Khriachtchev, L.; Lundell, J.; Räsänen, M. *J. Chem. Phys.* **2006**, *125*, 074501.
(40) Bochenkova, A. V.; Firsov, D. A.; Nemukhin, A. V. *Chem. Phys. Lett.* **2005**, *405*, 165.
(41) Jolkkonen, S.; Pettersson, M.; Lundell, J. *J. Chem. Phys.* **2003**, *119*, 7356.
(42) Bihary, Z.; Chaban, G. M.; Gerber, R. B. *J. Chem. Phys.* **2002**, *116*, 5521.

JP801363U